Atmos. Chem. Phys. Discuss., 12, 33083–33125, 2012
www.atmos-chem-phys-discuss.net/12/33083/2012/
doi:10.5194/acpd-12-33083-2012


Atmospheric Chemistry and Physics Discussions



# Dissolved organic carbon (DOC) and select aldehydes in cloud and fog water: the role of the aqueous phase in impacting trace gas budgets

**B. Ervens[1,2], Y. Wang[3], J. Eagar[3], W. R. Leaitch[4], A. M. Macdonald[4], K. T. Valsaraj[5], and P. Herckes[3]**

[1]Cooperative Institute for Research in Environmental Sciences, University of Colorado, Boulder, Colorado, USA
[2]Chemical Sciences Division, NOAA Earth System Research Laboratory, Boulder, Colorado, USA
[3]Arizona State University, Department of Chemistry and Biochemistry, Arizona, USA
[4]Air Quality Research Division, Atmospheric Science and Technology Directorate, Science and Technology Branch, Environment Canada, Downsview, Canada
[5]Cain Department of Chemical Engineering, Louisiana State University, Baton Rouge, LA, USA







Received: 29 October 2012 – Accepted: 9 December 2012 – Published: 19 December 2012

Correspondence to: B. Ervens (barbara.ervens@noaa.gov) and
P. Herckes (pierre.herckes@asu.edu)

Published by Copernicus Publications on behalf of the European Geosciences Union.





ACPD
12, 33083–33125, 2012



## Abstract

Cloud and fog droplets efficiently scavenge and process water-soluble compounds and thus modify the chemical composition of the gas and particle phases. The concentrations of dissolved organic carbon (DOC) in the aqueous phase reach concentrations on the order of $\sim 10\,\mathrm{mg\,C\,L^{-1}}$ which is typically on the same order of magnitude as the sum of inorganic anions. Aldehydes and carboxylic acids typically comprise a large fraction of DOC because of their high solubility. The dissolution of species in the aqueous phase can lead to (i) the removal of species from the gas phase preventing their processing by gas phase reactions (e.g. photolysis of aldehydes) and (ii) the formation of unique products that do not have any efficient gas phase sources (e.g. dicarboxylic acids).

We present measurements of DOC and select aldehydes in fog water at high elevation and intercepted clouds in a biogenically-impacted location (Whistler, Canada) and in fog water in a more polluted area (Davis, CA). Concentrations of formaldehyde, glyoxal and methylglyoxal were in the micromolar range and comprised $\leq 2\%$ each individually of the DOC. Comparison of the DOC and aldehyde concentrations to those at other locations shows good agreement and reveals highest levels for both in anthropogenically impacted regions. Based on this overview, we conclude that the fraction of organic carbon (dissolved and insoluble inclusions) in the aqueous phase comprises 1–$\sim 40\%$ of total organic carbon. Higher values are observed to be associated with aged air masses where organics are expected to be more highly oxidized and thus more soluble. Accordingly, the aqueous/gas partitioning ratio expressed here as an effective Henry's law constant for DOC ($K_{\mathrm{H}}^{*\mathrm{DOC}}$) increases by an order of magnitude from $7 \times 10^3\,\mathrm{M\,atm^{-1}}$ to $7 \times 10^4\,\mathrm{M\,atm^{-1}}$ during the ageing of air masses.

The measurements are accompanied by photochemical box model simulations. They suggest that the scavenging of aldehydes by the aqueous phase can reduce $HO_2$ gas phase levels by two orders of magnitude due to a weaker net source of $HO_2$ production from aldehyde photolysis in the gas phase. Despite the high solubility of dialdehydes






ACPD
12, 33083–33125, 2012



(glyoxal, methylglyoxal), their impact on the $HO_2$ budget by scavenging is $< 10\%$ of that of formaldehyde. The overview of DOC and aldehyde measurements presented here reveals that clouds and fogs can be efficient sinks for organics, with increasing importance in aged air masses. Even though aldehydes, specifically formaldehyde, only comprise $\sim 1\%$ of DOC, their scavenging and processing in the aqueous phase might translate into significant effects on the oxidation capacity of the atmosphere.

## 1 Introduction

The aqueous phase of clouds and fog constitutes a small volume of the atmosphere ($\sim 10^{-7}$ vol vol$^{-1}$) but can act as an efficient reservoir and reactor to convert soluble trace gases. Such soluble compounds include oxidation products of volatile organic compounds (VOC) that are emitted from anthropogenic or biogenic sources and are ubiquitous in the atmosphere. The most abundant organic compounds that have been identified in cloud and fog droplets are small volatile carboxylic acids (e.g. formic and acetic acid) as well as C1-C3 carbonyl compounds (Herckes et al., 2002b; Collett et al., 2008). Formaldehyde represents an end product in the oxidation chain of numerous VOCs and its gas phase mixing ratio exceeds that of other aldehydes by a factor up to 10 (Munger et al., 1995). However, dialdehydes, such as glyoxal or methylglyoxal, have higher Henry's law constants than formaldehyde has (by a factor of 10–100) resulting in similar aqueous phase concentrations as formaldehyde (e.g. Igawa et al., 1989; Munger et al., 1989). Simultaneous gas and cloud or fogwater measurements have shown that small aldehdyes are nearly in thermodynamic equilibrium whereas the aqueous phase appears to be enriched in larger compounds ($\geq$ C4) by up to a factor of 1000 (Munger et al., 1995; van Pinxteren et al., 2005; Li et al., 2008). The dissolved aldehyde fractions scale with the amount of total scavenged material that is removed by clouds and precipitation (Limbeck and Puxbaum, 2000; Maria and Russell, 2005; Li et al., 2008; Gong et al., 2011).





ACPD
12, 33083–33125, 2012



Oxidative processing of mono- and difunctional aldehydes in the aqueous phase leads to the formation of carboxylic acids that contributes to the acidity of rain water in remote regions (Khare et al., 1999). While the contributions of aqueous phase reactions to the total budgets of formic and acetic acids are not well constrained, it is established that aqueous phase processes represent the main source of keto- and dicarboxylic acids (Warneck, 2005). Many recent model, laboratory and field studies explored the role of aqueous phase reactions for the formation of such multifunctional acids since they remain in the particle phase upon droplet evaporation and contribute to ambient secondary organic aerosol (SOA) mass (e.g. Lim et al., 2010; Ervens et al., 2011; Lee et al., 2011). Less work has been dedicated to assessing the role of the aqueous phase of clouds and fogs as reservoir of dissolved organic carbon (DOC) and specifically aldehydes by evaluating their aqueous/gas partitioning.

The interaction of polar functional groups (e.g. carbonyl) with water molecules causes significant differences in their reactivity in either phase: While in the gas phase, oxidation and/or photolysis products of carbonyl compounds usually comprise small radicals from carbon-carbon bond breakage, hydration effects in the aqueous phase prevent such fragmentation and lead to functionalization of the reactants under retention of the carbon structure (e.g. carboxylic acid formation from aldehydes). There is evidence from a series of recent laboratory studies that carbonyl compounds might be also partially hydrated in the gas phase (Axson et al., 2010; Maroń et al., 2011). Due to the lack of observational data, this effect cannot be explored by means of model studies yet.

One of the most important net sources of the $HO_2$ radical in the atmosphere is the photolysis of formaldehyde in the gas phase (Finlayson-Pitts and Pitts, 2000):

$$HCHO + h\nu(+O_2) \rightarrow HO_2 + CHO \quad \text{(R1)}$$

$$CHO + O_2 \rightarrow HO_2 + CO \quad \text{(R2)}$$





ACPD
12, 33083–33125, 2012



The photolysis of other aldehydes such glyoxal and methylglyoxal also yields CHO and thus eventually to formation of $HO_2$ by (R3), followed by (R2).

$$RCHO + h\nu(+O_2) \rightarrow RO_2 + CHO \quad \text{(R3)}$$

Further reaction of the organic peroxy radical $RO_2$ eventually leads to HCHO; however, during that process $HO_2$ is consumed (R4) which leads to a net $HO_2$ yield of unity from reaction (R4) and (R5). Additional loss processes of the peroxides ROOH even decrease further this $HO_2$(g) yield from RCHO.

$$RO_2 + HO_2 \rightarrow ROOH \quad \text{(R4)}$$

$$ROOH + O_2 \rightarrow\rightarrow HCHO \quad \text{(R5)}$$

Since hydrated aldehyde (diol) groups do not undergo significant photolysis at atmospherically-relevant wavelengths, dissolved aldehdyes are not efficient $HO_2$ sources. Based on that, it has been shown that the uptake of formaldehyde into cloud droplets might have a sensitive impact on the atmospheric $HO_x$ budget (Lelieveld and Crutzen, 1991); the role of other aldehydes (e.g. glyoxal, methylglyoxal) has not been explored yet.

In addition to the aldehydes' role as direct $HO_2$ precursors, their different reactivities in gas and aqueous phases have further impacts on the $HO_x$ cycle: the rates of the OH reactions with dissolved aldehydes and their diols are usually higher than those of the corresponding gas phase aldehydes which can lead to an efficient removal of OH upon uptake into droplets (Monod et al., 2005). Indeed, it has been shown that the oxidation of hydrated formaldehyde by OH (and other organics) in cloud water is the main sink of dissolved OH in cloud droplets (Ervens et al., 2003a) and significantly contributes to the observed decrease in OH and other oxidant concentrations during cloud events (Frost et al., 1999; Morita et al., 2004). However, while Reactions (R1) through (R5) impact the absolute $HO_x$ budget, the faster OH reactions in the aqueous phase also yield $HO_2$ and accelerate the OH–$HO_2$ turnover.

In the current study, we present aqueous phase measurements of DOC and specific aldehydes (formaldehyde, glyoxal, and methylglyoxal) at two different locations:





ACPD
12, 33083–33125, 2012



(1) Cloud water was collected in Whistler (British Columbia, Canada), which represents a location that is impacted by a mix of anthropogenic and biogenic emissions. (2) Fog water was sampled in Davis (California), where the emissions originated from both biogenic and anthropogenic sources. These two data sets are discussed in the broader context of DOC and aldehyde concentrations and gas/aqueous partitioning at other locations that represent a wide spectrum of locations and emissions. Box model studies are performed to reproduce the observed aldehyde levels in the aqueous phase. While we do not attempt to simulate cloud/fog processing of aldehydes in detail, we rather apply the model to test our general understanding of trends in aldehyde aqueous phase concentrations. Based on additional, more exploratory simulations effects of aqueous phase aldehyde partitioning on gas-phase oxidant ($HO_2$) levels are estimated.

## 2 Experimental methods

### 2.1 Sampling locations

The "Whistler Aerosol and Cloud Study" (WACS2010) was conducted between 22 June and 28 July 2010 on Whistler Mountain, Whistler, British Columbia, Canada and aimed at exploring the interactions of biogenic emissions with clouds in a coniferous forest area. Chemical and microphysical measurements of the aerosol, gas and cloud phases were performed at mid-mountain (1300 m a.s.l.) and at the Whistler Peak (2182 m a.s.l.). Lidar measurements were conducted at mountain base (665 m a.s.l.). Macdonald et al. (2012) provide an extensive description of the study, the overall conditions and detailed information on measurements. A total of eight cloud events were sampled at Raven's Nest and three at the Peak site, some longer events yielded several cloud samples.

The second sampling location was in Davis, CA where a radiation fog field study was conducted between 6 January 2011 and 26 January 2011. Six fog events were sampled at the agricultural research station of the University of California, Davis. Emissions





ACPD
12, 33083–33125, 2012



in the wintertime are mainly impacted by vehicle traffic, biomass burning for heating purposes as well as some agricultural activities. More detailed information on the site, trace gas measurements and meteorological parameters is provided by Ehrenhauser et al. (2012).

## 2.2 Measurements

### 2.2.1 Liquid water content

In Whistler, cloud water samples were collected at Whistler Peak (mountain peak site) and at the Raven's Nest site (mid-mountain site) using an automated version of the Caltech Active Strand Cloud Water Collector (CASCC) (Demoz et al., 1996; Hutchings et al., 2010). Cloud Liquid Water Content (LWC) was measured using a Gerber Particulate Volume Monitor (Gerber PVM 100) (Gerber et al., 1991). The PVM data was used to trigger automated sampling.

In Davis, several CASCC type collectors were used for fogwater collection (e.g. Ehrenhauser et al., 2012). A Colorado State University Optical Fog Detector CSU-OFD was used (Carrillo et al., 2008) to trigger fog collection and provide semi-quantitative data. The obtained data could be used to assess relative trends in LWC and for detection purposes while absolute LWC values were inaccurate. LWC ranges that were used as input to the model simulations (Sect. 4) were derived from the volume of the collected fog samples, accounting for the collection efficiency (Ehrenhauser et al., 2012).

### 2.2.2 Chemical analysis of cloud and fog water samples

Identical methods to analyze the water samples were applied at both locations. Collected aqueous samples were weighed to determine collected water mass, then aliquotted for different chemical analyses. Fog or cloud sample pH was measured on site with a Denver Instruments IB-5 pH meter equipped with a Fisher Scientific Accumet gelfilled pH electrode, calibrated against pH 4 and 7 buffers.





ACPD
12, 33083–33125, 2012



Sample aliquots were prepared for major ion analysis by pipetting 1.5 mL of sample into a polypropylene auto-sampler vial and aliquots were stored refrigerated (4 °C) and in the dark until analysis at Arizona State University, immediately following the field study. Inorganic anion ($NO_3^-$, $NO_2^-$, $SO_4^{2-}$, and $Cl^-$) concentrations were determined using a Dionex DX-500 ion chromatograph equipped with an AG4A-SC guard column, AS4A-SC separation column, a Dionex Anion Self-Regenerating Suppressor (ASRS), and a conductivity detector. Separation was achieved using a 1.8 mM $Na_2CO_3$/1.7 mM $NaHCO_3$ eluent at a flow rate of 2.0 mL min$^{-1}$. Inorganic cation ($Na^+$, $NH_4^+$, $K^+$, $Mg^{2+}$ and $Ca^{2+}$) concentrations were determined using a second DX-500 ion chromatograph equipped with Dionex CG-12 and CS-12 guard and separation columns, a Dionex Cation Self Regenerating Suppressor (CSRS), and a conductivity detector. Separation was achieved using a 20 mM methanesulfonic acid eluent at a flow rate of 1.0 mL min$^{-1}$. Both IC systems were calibrated daily using a series of laboratory-prepared ion standards.

An aliquot of 30 mL of cloud or fogwater was preserved for aldehyde analysis by derivatization in the field immediately upon collection. The filtered fog water sample (30 mL) was transferred to a 40 mL amber vial with a Teflon lined septa cap. A citrate buffer solution (4 mL of pH 3) was added and pH was adjusted to 3 with HCl or NaOH, then 6 mL of dinitrophenylhydrazine (DNPH) reagent (3 g L$^{-1}$) was injected and heated (40 °C) on a stirring plate for two hours. The samples were refrigerated and transported to the laboratory for further processing. In the laboratory, the derivatized species were extracted with 20 mL dichloromethane for three times. Extracts were combined and 5 g anhydrous sodium sulfate was added then evaporated to a volume of 1 mL. Solvent was exchanged to acetonitrile and kept in a freezer until analysis.

Final sample extracts were analyzed using a Varian Prostar 210 HPLC system coupled to a Varian 335 Diode Array UV-Vis detector followed by a Varian 1200 L triple quadrupole mass spectrometric detector. Compound separation was performed using a Supelcosil LC18 (25 cm × 3 mm × 5 µm) column and gradient elution. Instrument and mass spectrometer-specific parameters are detailed in the Supplement (Tables S1 and





ACPD
12, 33083–33125, 2012



S2). Sample aliquots for dissolved organic carbon (DOC) analysis were filtered through glass fiber filters (VWR North America 691) in the field and stored in pre-baked amber glassware with a Teflon lined septa caps. The samples were stored refrigerated and analysis was performed immediately after completion of the field study. Both filtration and refrigerated storage minimized possible microbial activity in the samples. DOC concentrations were determined using a Shimadzu total organic carbon (TOC) analyzer (TOC-5000A) which was calibrated against potassium hydrogen phthalate standards.

### 2.3 Box model description

A photochemical box model is applied to simulate partitioning and processing of three aldehydes (formaldehyde, glyoxal, methylglyoxal) over short time scales (e.g. a few cloud/fog cycles). The formation of glyoxal and methylglyoxal is described by the gas phase oxidation of isoprene, toluene, benzene, xylene, based on the NCAR Master Mechanism (Madronich and Calvert, 1990; Stroud et al., 2003). Photolysis rates are adjusted to the respective locations and time of day (morning hours); it is assumed that photolysis rates are not affected by the presence of clouds/fog which might represent an overestimate of the photolysis rates in the interstitial spaces of optically thick clouds or their underestimate in the interstitial spaces in optically thin regions (Mayer et al., 1998; Tie et al., 2003). The aqueous phase oxidation mechanism of glyoxal and methylglyoxal has been developed in previous model studies (Ervens et al., 2004). The formation of formaldehyde is not explicitly simulated since primary sources of formaldehyde might be substantial and cannot be easily quantified (Lin et al., 2012). Unlike in previous model studies that addressed microphysical processes (e.g. cloud formation and evolution) in more detail (e.g. Ervens et al., 2004), in the current study, these processes are neglected and the total liquid water content (LWC) is distributed to a monodisperse drop population with a drop diameter of 10 µm.

Constant interaction between the gas and aqueous phases and chemical reactions in both phases are assumed for the whole simulation time (3 h). Simulations are performed for a range of liquid water contents ($0.05\,g\,m^{-3} < LWC < 0.3\,g\,m^{-3}$). This LWC





ACPD
12, 33083–33125, 2012



range covers the observed, highly variable LWCs in Whistler and Davis (Fig. 1). Since the model does not include any microphysical description of cloud (fog) evolution and precipitation, it cannot give detailed results in terms of the impact of the aqueous phase on the wet scavenging and removal of organic trace gases (e.g. Blando and Turpin, 2000; Yin et al., 2001; van Pinxteren et al., 2005). Because of the relative simplicity of the box model and uncertainties in initial values, we do not attempt to exactly reproduce observed concentration levels. Rather, the model is used to reproduce trends in aldehyde concentrations in the aqueous phase in Whistler and Davis and explore effects on predicted $HO_2$ concentrations in these two emission scenarios.

## 3 Results and discussion

### 3.1 Fog and cloud occurrence

The clouds sampled at Whistler Peak contained significantly more water (LWC $\leq$ 1 g m$^{-3}$) than the fogs in Davis where the average LWC was $<$ 0.1 g m$^{-3}$ (0.019–0.086 g m$^{-3}$ based on the collected volumes of water; Fig. 1), in general agreement with the higher cloud LWC as compared to fogs (Seinfeld and Pandis, 1998). In Davis, for part of the study, the optical fog detector yielded qualitative data (detection of fog events) rather than quantitative data (Ehrenhauser et al., 2012). In Whistler, cloud samples were collected both at day and at night time. The local topography with upslope/downslope winds made it impossible to clearly differentiate between intercepted cumulus or orographic clouds. One sample obtained at Whistler Peak (evening to morning), and seven samples from Raven's Nest were prepared for carbonyl analysis, four of which were collected during daylight while three were collected during partial day and partial night time. The sampling times ranged from 1.25 to 15 h; most were less than two hours.

In Davis, radiation fogs typically formed in the evening or at night and lasted through the morning hours although one event persisted throughout the day at low LWC





ACPD
12, 33083–33125, 2012



(Ehrenhauser et al., 2012). Eight of the samples were analyzed for carbonyl compounds – of which four were night samples, three were daylight samples and one was an evening sample. The corresponding sampling times varied from 2.5 to 8 h.

### 3.2 Dissolved organic carbon (DOC)

The DOC concentrations in the Whistler cloud study ranged from 1.8 to 5.8 mg C $L^{-1}$ at Raven's Nest and 3.1–8.1 mg C $L^{-1}$ at the Peak site (Fig. 2a). Except for the July 11 event which showed a very high DOC concentration at the Peak, all concentrations were similar at the Peak site and at Raven's Nest. The DOC concentrations in the radiation fogs in Davis were generally higher than in Whistler and ranged from 5.9 to 27 mg C $L^{-1}$ with a median value of 12.6 mg C $L^{-1}$ (Fig. 2b). In general, DOC concentrations reflect the abundance of VOCs and carbonaceous particles in the atmosphere and, thus, as expected the observed levels in Whistler are in the lower range of observed concentrations in continental clouds (Table 1; Fig. 2c). Although the atmosphere at Whistler can contain substantial concentrations of VOCs and organic aerosol, they are largely from biogenic sources and consequently strong functions of temperature (e.g. Leaitch et al., 2011); during 2010, the clouds sampled were mostly during cooler periods (Macdonald et al., 2012).

Figure 2c summarizes DOC levels in cloud and fog water from previous studies at various locations and shows that the present observations fall within the spread of the concentrations reported. DOC sampled in fog water in Davis was at the lower end of observations in the Central Valley of California with a median higher than in rural Angiola but clearly lower than in the larger urban areas of Fresno and Bakersfield. The concentrations were slightly higher than observations in rural Pennsylvania but lower compared to Po Valley studies. DOC concentrations in Whistler were on the lower end for reported cloud observations. DOC was lower than in more polluted environments including US East Coast, Europe or China. The highest DOC values in Whistler ($\sim$ 10 mg $L^{-1}$) are higher than the average values in the more anthropogenically-impacted locations since the strong biogenic sources in Whistler are significant organic





ACPD
12, 33083–33125, 2012



carbon sources. In general, it has been found that DOC constitutes about 80 % of the total organic carbon (TOC) in the aqueous phase (Herckes et al., 2002a; Raja et al., 2008; Straub et al., 2012); thus, DOC is a nearly quantitative measure of TOC in the condensed phase of clouds and fogs.

In order to estimate the fraction of DOC to the total organic carbon, a measure is needed that quantifies total organic carbon in the atmosphere. A comprehensive summary of the ambient total observed organic carbon (TOOC) (gas and particulate; no clouds) over North America is given by Heald et al. (2008): concentrations reach from $\sim 5\,\mu g\,m^{-3}$ in remote areas (Trinidad Head) to $> 40\,\mu g\,m^{-3}$ in large cities (e.g. Pittsburgh and Mexico City). TOOC excludes methane and includes all other organic carbon that can be detected by standard techniques, but might miss semivolatile compounds with multiple functional groups. The analysis by Heald et al. (2008) reveals that small compounds ($\leq C_3$) that are easily accessible by routine measurements contribute to a significant fraction of all measured organics and, thus, TOOC likely captures the major fraction of the total organic carbon that is present in the atmosphere. The ratio of aerosol to gas phase OC ($OC_p/OC_{gas}$) varies from $\sim$ 6–46 % with a median value of 14 % (Fig. 6a in Heald et al., 2008). Based on this median ratio, the fraction of OC that is associated with the particle phase can be calculated as $F(OC_p)=OC_p/(OC_p + OC_{gas})=12.3\,\%$ $(0.14/1.14 \cdot 100\,\%)$ whereas the denominator represents TOOC.

Since $F(OC_p)$ is not directly available from the measurements listed in Table 1, we apply this $F(OC_p)$ value of 12.3 % to obtain an estimate of TOOC based on $OC_p$ measurements. Using these TOOC values, the ratio of the aqueous (DOC) and gas phase concentrations can be derived. We express the ratio in the following as an overall effective Henry's law constant for DOC

$$K_H^{*DOC} = \frac{DOC\,[mol\,L_{aq}^{-1}]}{OC_{gas}\,[atm]} \quad (1)$$





ACPD
12, 33083–33125, 2012



Details on the calculation are given in the supplemental information. Given that DOC represents the major fraction of all organic carbon in the aqueous phase, $K_H^{*DOC}$ can be considered an approximate measure of the partitioning of TOC between the condensed phases of cloud/fog water and the gas phase.

The resulting $K_H^{*DOC}$ ($7000 < K_H^{*DOC}$ [M atm$^{-1}$] $< 71000$; Table 1) are in general agreement with Henry's law constants for monofunctional compounds, such as formaldehyde ($K_H$ [M atm$^{-1}$] $= 2970 \cdot [7216 \cdot \exp(1/T\,[\mathrm{K}] - 1/298)]$, Betterton and Hoffmann, 1988) or formic acid ($K_H$ [M atm$^{-1}$] $= 3700 \cdot \exp[5700 \cdot \exp(1/T\,[\mathrm{K}] - 1/298)]$; at pH = 4, Chameides, 1984) which might support the general finding that DOC is mostly composed of such species. However, they are much lower than the value that has been derived for gas/particle partitioning of water-soluble organic carbon ($c_p/p_g = K_H^{*WSOC} \sim 2 \times 10^9$ M atm$^{-1}$, Hennigan et al., 2009) in the absence of clouds. This trend is in agreement with results for the gas/particle partitioning of individual highly polar compounds that show significantly greater partitioned fractions than predicted based on Henry's law constants (Baboukas et al., 2000; Matsunaga et al., 2005; Healy et al., 2008).

Based on $K_H^{*DOC}$, the fraction of organic carbon can be derived that is dissolved in the aqueous phase of cloud/fog droplets ($F(OC_{aq})$). These values show that the carbon fraction dissolved in cloud water is ~ 1–46 % depending on location (Table 1). The amount of water associated with non-activated particles (in interstitial spaces or in the absence of clouds) is smaller by several orders of magnitude than that of cloud droplets (LWC (particles) ~ 10 µg m$^{-3}$ vs LWC (clouds) ~ 0.1 g m$^{-3}$). In such particles, the volume of the water phase where soluble species are dissolved is comparable to that of (an) organic phase(s) where less water-soluble, more hydrophobic organics might be absorbed. Thus, the fraction of organics associated with the particle phase does not necessarily correlate with the particle LWC. In clouds, the aqueous phase represents by far the largest condensed phase and thus the fraction of organics dissolved in the aqueous phase exceeds that of all other organics. While it is likely that a large fraction of particulate organic carbon is dissolved in droplets that formed on organic condensation nuclei, $F(OC_{aq})$ may also be enhanced by dissolution of soluble organic gases





ACPD
12, 33083–33125, 2012



too volatile to be associated with particles outside of clouds/fogs. While we have used an average value of 14 % for $OC_p$/TOOC, in the original study this value shows considerable variability (6–32 %) (Heald et al., 2008). The lowest value (6 %) was observed in Pittsburgh where 66 % of the organic aerosol fraction was classified as oxygenated organic aerosol (OOA) and can be considered as water-soluble (Zhang et al., 2005). The maximum value was derived in more aged air masses at Chebogue Point where the organic aerosol fraction was nearly completely oxygenated (Ervens et al., 2007). OOA is usually associated with accumulation mode particles that can be activated into droplets where water-soluble constituents will dissolve. If all OOA in Pittsburgh and Chebogue Point were to dissolve in water, resulting $F(OC_{aq})$ of ~ 4 % and 32 % were obtained. These values are in general agreement with $F(OC_{aq})$ for relatively fresh and more aged air masses in Table 1. This estimate suggests that most of the DOC originates from dissolved $OC_p$ and the uptake of water-soluble gases only contributes to a smaller extent.

The data in Table 1 are sorted by the $OC_p$ mass concentration, as a proxy for pollution level. The majority of the locations listed in Table 1 are impacted by anthropogenic emissions. However, the relatively high $OC_p$ in Whistler is mostly due to biogenic compounds. Despite the uncertainty associated with the estimate in TOOC, the fractions and $K_H^{*DOC}$ values show a trend with decreasing particulate organic carbon mass. The organic fraction in the aqueous phase is lowest at Fresno, CA, where highly polluted radiation fog was sampled. Organics were not aged and thus their solubility was limited (reflected by the relatively low $K_H^{*DOC} = 7000\,M\,atm^{-1}$). Locations with lower $OC_p$ concentrations generally show higher organic fractions in the aqueous phase. This trend can be explained by the fact that polluted air masses are usually diluted during transport leading to lower $OC_p$ loadings. During transport and ageing, organics become oxidized which translates into higher solubility which in turn leads to higher dissolved fractions. The highest fraction of organic material in the aqueous phase related to total organics (gas + dissolved) is estimated to have been present in clouds at Whiteface Mountain. While the LWC there was highest among all locations listed in Table 1, this factor alone





ACPD
12, 33083–33125, 2012



cannot account for the significantly higher fraction of organics that is dissolved (46 %). The higher solubility associated with more aged air masses is also reflected in the trend of $K_H^{*DOC}$ (Eq. 1; and Supplement) as it increases from $K_H^{*DOC} = 7000\,M\,atm^{-1}$ for the fresh air masses in Fresno to $K_H^{*DOC} = 71000\,M\,atm^{-1}$ in the most aged air masses at Whiteface Mountain. Similar trends have been observed for the degree of oxygenation of organic aerosol particles that usually show enhanced amounts of highly oxidized material in aged air masses whereas the inferred ageing does not necessarily occur in the aqueous phase (e.g. Ng et al., 2011).

### 3.3 Aldehydes in cloud and fog water

#### 3.3.1 Aqueous phase concentrations and their ratios

Figure 3a shows the concentrations of individual aldehydes observed during the two studies. At Raven's Nest (Whistler), the sum of all aldehyde concentrations included in this study ranges from 12 to 25 µM. The most abundant aldehyde was formaldehyde which ranged from 3.8–10.4 µM. Formaldehyde was followed by acetaldehyde, propionaldehyde and valeraldehyde. Glyoxal and methylglyoxal concentrations were typically lower than formaldehyde and acetaldehyde but still on the same order of magnitude. The four carbonyl and two dicarbonyl compounds contribute each about 2–3 % to the identified DOC on average. In Davis, the data set is limited to formaldehyde, glyoxal and methylglyoxal. Formaldehyde was typically the most abundant aldehyde with concentrations from 5.5 to 7.3 µM. Concentrations of glyoxal were more variable (1.3 to 8.7 µM). Methylglyoxal concentrations were lower with concentrations of 0.1–0.9 µM. Overall these aldehydes contribute < 1 % to the identified DOC in Davis. This trend is agreement with the findings in Table 1 that imply a smaller fraction of highly soluble species, such as aldehydes, to DOC.

Figure 3b compares the observed aldehyde concentrations in Whistler and Davis to corresponding measurements at other locations. In agreement with higher VOC emissions in more polluted scenarios, the aldehyde concentrations differ by more than two





ACPD
12, 33083–33125, 2012



orders of magnitude between the most polluted (Riverside) and the most remote location (Whistler) whereas the latter was strongly impacted by biogenic emissions. For any given location, the aqueous phase concentrations are mostly within the same order of magnitude for the three aldehydes despite their greatly different gas phase levels (not measured in Whistler and Davis): in Virginia, median formaldehyde levels of 755 ppt were found and significantly smaller glyoxal and methylglyoxal mixing ratios (22 ppt, < 50 ppt, respectively) (Munger et al., 1995). At the Schmücke (Germany), formaldehyde, glyoxal and methylglyoxal mean mixing ratios ranged from 480–940 ppt, 1–23 ppt, and 17–75 ppt, respectively, depending on time of day and wind direction (Müller et al., 2005). The Henry's law constants of glyoxal and methylglyoxal are approximately two and one order of magnitude higher than that of formaldehyde, respectively ($K_{H,Glyoxal} = 4.19 \times 10^5 \cdot \exp[(6200/R) \cdot (1/T\,[K] - 1/298)]$, Ip et al., 2009; $K_{H,Methylglyoxal} = 32\,000\,M\,atm^{-1}$, Zhou and Mopper, 1990; $K_{H,Formaldehyde} = 2970 \cdot \exp[(59800/R) \cdot (1/T\,[K] - 1/298)]\,M\,atm^{-1}$, Betterton and Hoffmann, 1988). Assuming thermodynamic equilibrium, these differences in solubility result in predicted dissolved fractions of 50 %, 5 % and ~ 1 % for the three aldehydes for an LWC = 0.1 g $m^{-3}$ (Fig. 4), whereas the resulting aqueous phase concentrations of all three aldehydes are on the same order of magnitude (Fig. 3).

The total concentration levels of the aldehydes depend on the precursor mixtures which are vastly different between anthropogenic (e.g. Riverside) and more biogenically-impacted (e.g. Whistler) locations. While the glyoxal and methylglyoxal yields from toluene are approximately equal (24 % and 19 %, respectively, at low $NO_x$ level), methylglyoxal yields from o- and m-xylene exceed the ones of glyoxal by a factor of ~ 4 (~ 10 % and ~ 40 %, respectively) (Nishino et al., 2010). Glyoxal and methylglyoxal are not only first- but also second generation products in the oxidation of isoprene and thus their concentration ratio changes over time depending on the availability of oxidants. In general, the overall yields of these aldehydes from isoprene are much lower than those from the oxidation of aromatics (<~ 2 % glyoxal yield, ~ 20 % methylglyoxal yield from isoprene, Galloway et al., 2011). Whistler is the location that





ACPD
12, 33083–33125, 2012



is most strongly impacted by biogenic emissions, thus the main glyoxal and methylglyoxal precursor is expected to be isoprene. The photolysis rates and second-order rate constants for the OH reactions in the gas phase differ by less than a factor of two for both dialdehydes, respectively ($j_{Gly} = 8 \times 10^{-5}\,s^{-1}$; $j_{Mgly} = 1.2 \times 10^{-4}\,s^{-1}$ (based on the TUV model, as described, e.g. in Tie et al., 2003); $k_{OH,Gly} = 1.15 \times 10^{-11}\,cm^3\,s^{-1}$; $k_{OH,Mgly} = 1.75 \times 10^{-11}\,cm^3\,s^{-1}$, Plum et al., 1983). In the aqueous phase, the ratio of the second-order rate constants for the OH reactions of both dialdehydes is similar ($k_{OH,Gly} = 1.1 \times 10^9\,M^{-1}\,s^{-1}$ (Buxton et al., 1997); $k_{OH,Mgly} = 6.2 \times 10^8\,M^{-1}\,s^{-1}$, Schaefer et al., 2012). Thus, the loss terms of the aldehydes are similar when they are exposed to identical air masses. The differences in the concentration ratios of glyoxal to methylglyoxal in the aqueous phase (less than unity in Whistler, greater than unity at all other locations, Fig. 3b) can be explained by the higher methylglyoxal yields from isoprene as compared to glyoxal. In addition, in more aged air masses the more soluble glyoxal might have been preferentially removed by scavenging and processing in the condensed phase.

### 3.3.2 Gas/aqueous phase partitioning of aldehydes

There are only a few data sets available that report simultaneous measurements of aldehydes in both phases, gas and aqueous. In orographic clouds at the Schmücke (Germany), it was found that the partitioning of formaldehyde, glyoxal and methylglyoxal between the aqueous and gas phases corresponds to $c(aq)/p(g) = \sim 3000\,M\,atm^{-1}$; $\sim 2 \times 10^5\,M\,atm^{-1}$ and $3 \times 10^4\,M\,atm^{-1}$, respectively (van Pinxteren et al., 2005). Similar ratios can be also calculated for the partitioning of these compounds observed in Virginia (Munger et al., 1995) and for formaldehyde during the ICARTT campaign (Li et al., 2008). These ratios are very close to the Henry's law constants ($K_{H,298\,K}$(Glyoxal) = $4.19 \times 10^5\,M\,atm^{-1}$ (Ip et al., 2009); $K_{H,298\,K}$(methylglyoxal) = $3.2 \times 10^4\,M\,atm^{-1}$ in sea water, Zhou and Mopper, 1990). For methylglyoxal, the Henry's law constant is significantly smaller in pure water ($2970\,M\,atm^{-1}$; Betterton and Hoffmann,





ACPD
12, 33083–33125, 2012



1988) while ionic effects do not seem to significantly affect the constant for glyoxal. The assumption of cloud water being an ionic solution appears to be justified since it comprises many inorganic and organic compounds at micro- and up to tenths of millimolar concentrations. While the aforementioned studies analyzed bulk water samples, size-resolved measurements have shown enhanced formaldehyde concentrations (by a factor of $\sim 1.5$) with decreasing droplet size. This trend has been explained by the kinetic limitation of formaldehyde uptake into larger droplets (Ervens et al., 2003b).

The fraction of aldehydes that is predicted to be present in the aqueous phase is shown in Fig. 4. It is evident that only for the highly soluble glyoxal the dissolved fraction might reach a maximum of $\sim 70\,\%$ (at LWC $\geq 0.1\,\mathrm{g\,m^{-3}}$) whereas the dissolved fraction of the less soluble aldehydes does not exceed 10 % at any reasonable LWC. While these aldehydes will evaporate during drop evaporation, their different reactivities in the gas and aqueous phases also impact the aldehydes budgets to different extents: assuming day time OH concentrations of $\sim 10^6\,\mathrm{cm^{-3}}$ and $10^{-13}\,\mathrm{M}$ in the gas and aqueous phases, respectively, the first order loss rates for aldehydes ($k^{1st} = k^{2nd}$ [OH]) are on the order of $k^{1st}_{gas} = 10^{-5}\,\mathrm{s^{-1}}$ ($10^{-11}$ cm$^3$ s$^{-1}\cdot$ $10^6$ cm$^{-3}$) and $k^{1st}_{aq} = 10^{-4}$ s$^{-1}$ ($\sim 10^9$ M$^{-1}$ s$^{-1}\cdot$ $10^{-13}$ M). Considering that there are several dark sources of OH in the aqueous phase (e.g. Fenton reactions, Ervens et al., 2003a) the ratio of the loss rates in the gas and aqueous phase will be even higher during early morning when most of the fog and cloud samples were acquired. Thus, the aqueous phase does not only act as a reservoir for aldehydes and protects them from being photolyzed but it also represents a significant sink for aldehydes due to the efficient consumption that affects their overall concentrations.

In addition to hydration that is implicitly included in the Henry's law constants, aldehyde partitioning can be further shifted towards the aqueous phase by the formation of adducts with sulfur(IV) (Olson and Hoffmann, 1989):

$$\mathrm{RCH(OH)_2 + HSO_3^- \Leftrightarrow RCH(OH)SO_3^-} \qquad \text{(R6)}$$





ACPD
12, 33083–33125, 2012



The overall partitioning of aldehydes can be then calculated based on the equilibrium constants for (R6) for formaldehyde ($K_{SIV,HCHO} = 3.6 \times 10^6\,M^{-1}$), glyoxal ($K_{SIV,Gly} = 2.8 \times 10^4\,M^{-1}$), and methylglyoxal ($K_{SIV,Mgly} = 3.1 \times 10^5\,M^{-1}$) (Olson and Hoffmann, 1989). Similar to the expression for an effective Henry's law constant that includes hydration (Betterton and Hoffmann, 1988), the partitioning of total aldehyde (aldehyde + hydrated aldehyde + sulfur(IV) adduct) can be expressed as

$$K_H^{SIV} = \frac{[RCH(OH)_2 + RCH(OH)SO_3^-]_{aq}}{RCHO_{gas}} \quad (2)$$

Similar to our definition of $K_H^{*DOC}$, this $K_H^{SIV}$ does not follow strictly the definition of a Henry's law constant as it includes chemical conversion in addition to hydration. Rearranging Eq. (2) and substituting

$$[RCH(OH)SO_3^-] = K_{SIV,RCHO} \cdot [RCH(OH)_2] \cdot [S(IV)]_{aq} \quad (3)$$

yields

$$K_H^{SIV} = K_{H,Hydr} \cdot (1 + K_{SIV,RCHO} \cdot [S(IV)]_{aq}) \quad (4)$$

whereas $[S(IV)]_{aq}$ is the total $HSO_3^-$ + $SO_3^{2-}$ concentration in the aqueous phase. Thus, a significant enhancement in aldehyde partitioning beyond that suggested by $K_H$ (including hydration) is only expected if $[S(IV)]_{aq} \gg K_{SIV,RCHO}$. Based on the average $SO_2$ concentrations and pH values of the cloud/fog water in Whistler ($SO_2 \leq 0.3$ ppb; pH ~ 4.4), and from past measurements in Davis ($SO_2 \leq 1$ ppb, pH ~ 6, Reilly et al., 2001), concentrations of $[S(IV)] \sim 4\,\mu M$ and $17\,\mu M$, respectively, can be calculated for the two locations. A comprehensive overview of sulfite measurements shows that only at very polluted locations, sulfite concentrations exceed ~ 20 mM and substantial sulfonate formation can be expected (Rao and Collett, 1998). At all other locations, the fraction of formaldehyde that is present as hydroxy methanesulfonate is < 5%. Since





ACPD
12, 33083–33125, 2012



the $K_{SIV,RCHO}$ for glyoxal and methylglyoxal are one and two orders of magnitude smaller, it can be concluded that (R6) does not significantly enhance aldehyde partitioning in the aqueous phase. In addition, it should be noted that Eq. (2) only accounts for equilibrium. However, it has been shown that the adduct formation is relatively slow (Betterton et al., 1988; Olson and Hoffmann, 1989) and only under very high S(IV) concentrations and in large droplets, deviations from thermodynamic equilibrium due to aldehyde-S(IV) interactions might be expected (Ervens et al., 2003b). Based on these estimates, sulfonate formation is not included in the following box model studies.

## 4 Box model results

### 4.1 Predicted trends in aqueous phase concentrations of glyoxal and methylglyoxal

The box model as described in Sect. 2.3 was initialized with mixing ratios of VOCs and oxidants ($NO_x$, $O_3$) taken from the respective field experiments (Table 2). Box model results are presented as a function of LWC and processing times. In order to cover the LWC range observed in the two field studies, multiple model simulations are performed with a constant LWC in each simulation. While a cloud or fog event might last several hours, the lifetime of a single droplet is usually restricted to a few minutes upon which volatile gases, such as aldehydes, will evaporate together with water. Thus, the processing time of volatile aldehydes is restricted to the time of the formation/evaporation cycle of a single droplet. Multiple cycles might occur on the same particle during a cloud event but the exact processing time in a single cloud droplet is a measure that is not easily accessible from measurements. Thus, a processing time of several hours might represent several cloud/fog cycles but the exact cloud contact time or number of drop formation/evaporation cycles cannot be derived from measurements.

A first set of model results shows the predicted aqueous phase concentrations for the three aldehydes (Fig. 5). Predicted formaldehyde concentrations are nearly identical for





ACPD
12, 33083–33125, 2012



both locations with only a weak impact of processing time. Predicted glyoxal concentrations are smaller by nearly one order of magnitude in Whistler as compared to Davis, in approximate agreement with observations ($\sim 3\,mg\,L^{-1}$ vs. $\sim 0.5\,mg\,L^{-1}$; Fig. 3a). Predicted methylglyoxal concentrations are very similar for both locations, which together with the greatly varying glyoxal concentrations result in concentration ratios that are similar to the observed ones, i.e. glyoxal/methylglyoxal ratios less than unity in Whistler and exceeding unity in Davis. These trends can be explained by the different yields of glyoxal and methylglyoxal by typical anthropogenic and biogenic precursors: the ratios of glyoxal to methylglyoxal molar yields in the gas phase as determined in chamber studies are greater than unity for toluene and p-xylene and slightly smaller than unity for other substituted monoaromatics (Nishino et al., 2010). Benzene is often one of the most abundant aromatic and only yields glyoxal. As it can be expected from these yields and their ratios, in anthropogenically influenced regions, the glyoxal/methylglyoxal ratios are near unity (Fu et al., 2008). Isoprene shows much higher methylglyoxal concentrations than glyoxal (Galloway et al., 2011) and thus in biogenically-impacted regions, the ratio of glyoxal to methylglyoxal is much smaller ($\sim 0.2$) (Spaulding et al., 2003).

In general, the predicted and observed aqueous phase concentrations of glyoxal and methylglyoxal in Whistler are much lower compared to other locations (Fig. 3b). Many recent model and laboratory studies have predicted efficient formation of secondary organic aerosol from glyoxal and methylglyoxal in the aqueous phase (Ervens et al., 2011 and references therein). For the relatively clean conditions in Whistler, mass concentrations of SOA on the order of $10\,ng\,m^{-3}$ are predicted upon processing times of several hours which might correspond to many cloud cycles (results not shown). Such small changes in total aerosol mass might be below the detection limit. These results appear to be in contradiction to results from a recent laboratory study where efficient SOA formation in Whistler was predicted (Lee et al., 2012) but they rather agree with findings of efficient organic aerosol oxidation by OH that leads to a decrease in total organic aerosol mass (Slowik et al., 2012). It should be noted that the study by Lee et al. (2012) was performed on highly concentrated cloud samples under the influence of increased





ACPD
12, 33083–33125, 2012



OH concentrations. These experimental conditions might overestimate SOA formation and do not reflect the limited time scales as encountered in cloud droplets that undergo quick formation and evaporation cycles. In summary, the box model applied here is able to represent concentration levels of the three aldehydes in the aqueous phase. This general agreement gives confidence that it is suited to conceptually simulate trends in concentration levels and ratios in the multiphase system despite uncertainties in initial conditions and details on cloud/fog microphysical parameters and evolution.

### 4.2 Impact of aldehyde scavenging on $HO_2$

Gas phase photolysis of formaldehyde represents the major $HO_2$(g) source and thus the initiator of the $HO_x$ cycle (R1). The photolysis rates of the different aldehydes in the gas phase differ by roughly a factor of four, with formaldehyde having the smallest and methylglyoxal having the largest value ($j_{HCHO} \sim 4 \times 10^{-5}\,s^{-1}$; $j_{Gly} = 8 \times 10^{-5}\,s^{-1}$; $j_{Mgly} = 1.2 \times 10^{-4}\,s^{-1}$ for the photochemical conditions in Whistler). In order to predict exemplary the impact of aldehyde partitioning on $HO_2$ gas phase concentrations in the presence and absence of clouds, simulations are performed for a processing time of 30 min and LWC = 0.1 g m$^{-3}$ which roughly represent a lower LWC limit in clouds and an upper limit for fog LWC (Fig. 1). Two sets of simulations are compared, i.e. one that considers a pure gas phase system without any partitioning to and processing in the aqueous phase whereas the second uses the multiphase system as applied in Fig. 5.

Figure 6a shows that under mostly biogenic conditions (Whistler), $HO_2$(g) levels can be reduced by up to two orders of magnitude (−96 %) in the presence of clouds. This difference is in general agreement with detailed multiphase model simulations that explored the effects of aqueous phase chemistry on organic peroxy radical levels (Herrmann et al., 2005). The decrease is smaller (−44 %) in more polluted conditions as encountered in Davis since the oxidation of CO is relatively more important in terms of $HO_2$ production due to higher CO levels.

$$CO + OH\,(+\,O_2) \rightarrow CO_2 + HO_2 \qquad \text{(R7)}$$





ACPD
12, 33083–33125, 2012



In addition, more complex chemical feedbacks are occurring that affect the oxidant cycles, such as the faster turnover of OH into $HO_2$ due to the higher reaction rate of hydrated formaldehyde in the aqueous phase as compared to the corresponding gas phase process.

In Fig. 6b, the reduction in $HO_2$(g) concentration is shown whereas we define these changes as

$$\Delta HO_2 = \left(1 - \frac{HO_2 \text{ in presence of aqueous phase}}{HO_2 \text{ in absence of aqueous phase}}\right) \cdot 100\,\% \quad (5)$$

The bars on the left hand side of Fig. 6b ("base case") repeat the results of Fig. 6a. In order to investigate which aldehyde has the strongest impact on the $HO_2$ decrease, three additional exploratory simulations were performed in which the uptake of a single aldehyde is excluded from the multiphase mechanism. These simulations allow us to understand feedbacks in the multiphase system in a simplified manner. The results of these simulations are shown in the right hand part of Fig. 6b. Excluding the uptake of formaldehyde leads to $HO_2$(g) concentrations that are 70 % (Whistler) and 11 % (Davis) smaller than results of simulations that include its uptake and subsequent aqueous phase processing. The results from the other cases where the uptake of glyoxal or methylglyoxal are ignored show that the dissolution of either aldehyde only affects $HO_2$(g) levels marginally (< 1 %). Even though the fraction of glyoxal scavenged is the highest (Fig. 4), its relative role as $HO_2$(g) precursor seems least important since its photolysis rate is roughly a factor of two smaller than that of methylglyoxal. It is not expected that the sum of the bars in the set of three simulations in Fig. 6b add up to the total decreases as shown on the left-hand side since neglecting the uptake of a single aldehyde into the aqueous phase causes non-linear feedbacks on oxidant concentration levels that impact oxidation rates in both phases. In general, these trends show that even though the aqueous phase is a more effective reservoir for the difunctional compounds (Fig. 4), their importance as $HO_2$ precursor is much smaller due to their smaller gas phase concentrations and less efficient formation of $HO_2$ (R3–R5). Our approach of using identical photolysis rates within and outside clouds might be somewhat





ACPD
12, 33083–33125, 2012



simplified as within optically thick clouds photolysis rates tend to be lower whereas they might be enhanced due to reflection on droplets in optically thinner regions of clouds, i.e. near their edges. The extent to which these opposite effects might possibly lead to a (partial) cancellation of the change in photolysis rates will depend on cloud properties (thickness, droplet distributions etc). In addition to the cloud impacts on photolysis rates, it might be possible that gas phase aldehyde concentrations near cloud edges are enhanced from evaporating cloud droplets which might even enhance further $HO_2$ production. For simplicity, these effects are not considered in our box model. However, it can be expected that they might affect the levels of all aldehydes to a similar extent and thus it is concluded that the trends shown in Fig. 6 are robust.

These model results generally confirm conclusions by Lin et al. (2012) on the total $HO_x$ budget that have been drawn based on formaldehyde measurements: it was found that formaldehyde photolysis contributes ~ 18 % to the total $HO_x$ budget, only exceeded by HONO (67 %) and followed by $O_3$ photolysis and alkene reactions with ozone (13 % and 2 %, respectively). While these numbers are not directly comparable to our model results since we do not discuss any impacts on the OH budget, the fact that in the study by Lin et al. (2012) no other aldehydes were identified as significant contributors to the $HO_x$ budget is in agreement with our findings that glyoxal and methylglyoxal – as proxies for higher aldehydes – likely play a minor role.

Our model results suggest that the dissolution and subsequent hydration of aldehydes can significantly impact $HO_2$ levels and ultimately the oxidant cycles in the multiphase system. The estimated scavenged carbon fractions (~ 1 % < DOC/TOOC <~ 46 %) and the quantification of aldehydes as contributors to DOC ($[\text{formaldehyde} + \text{glyoxal} + \text{methylglyoxal}]_{aq}/\text{DOC} \sim 6\,\%$) imply that even scavenging of a very small organic carbon fraction (< 1 %) might lead to significant changes in the oxidant budget of the atmosphere. This fraction only represents the partitioning at a given time but in the dynamical multiphase system, aldehydes are quickly consumed in the aqueous phase and thus affect the aldehyde levels in both the gas and aqueous phases. The extension of our study to difunctional aldehydes exceeds early findings on the role of clouds in





ACPD
12, 33083–33125, 2012



impacting $HO_2$ by removal of formaldehyde by aqueous phase processes (Lelieveld and Crutzen, 1991). Since the three aldehydes comprise only about 6 % of the total identified dissolved aldehydes in cloud and fog waters, it might be expected that the total effects of aldehyde hydration in the aqueous phase on $HO_2$ levels could be even greater.

## 5 Conclusions

Dissolved organic carbon (DOC) and select carbonyl species were measured in clouds collected in Whistler and fog in Davis (CA). Formaldehyde, glyoxal and methylglyoxal were present in the micromolar concentration range and accounted for up to 10 % of the dissolved organic carbon. DOC concentrations were lower in Whistler compared to Davis and were consistent with literature data at similar locations. An overview of different data sets reveals that DOC as well as carbonyl concentrations increase from remote to polluted environments. The overall solubility (expressed here as an effective Henry's law constant $K_H^{*DOC}$) that describes the distribution of organic carbon between the aqueous and gas phases shows an increase with increasing distance to pollution sources ($7000\,M\,atm^{-1} < K_H^{*DOC} < 71\,000\,M\,atm^{-1}$). This trend points to a greater fraction of oxidized organic material and a higher partitioned carbon fraction in aged air masses. Indeed the aqueous phase carbon fraction increases from ~ 1 % in fog in highly polluted areas to ~ 46 % in more remote locations. In the gas phase, formaldehyde is the predominant aldehyde and its concentration exceeds those of dialdehydes approximately by an order of magnitude. However, the solubility (Henry's law constant) of the dialdehydes is greater by one (methylglyoxal) and two (glyoxal) order of magnitude, respectively. Thus, dialdehydes are more efficiently dissolved in the aqueous phase; it is predicted that at a liquid water content of $0.1\,g\,m^{-3}$, ~ 70 % of glyoxal, ~ 5 % of methylglyoxal and 1 % of formaldehyde are present in the aqueous phase. These different dissolved fractions of the aldehydes can explain similar concentration levels (~ µM) of these three aldehydes in the aqueous phase of fog and cloud droplets.





ACPD
12, 33083–33125, 2012



The observed formaldehyde, glyoxal and methylglyoxal concentrations in cloud water as observed in Whistler and Davis can be reproduced reasonably well by box model simulations that are initialized with measured VOC precursor concentrations and liquid water contents. Model results also show that the dissolution of formaldehyde has the greatest impact on predicted $HO_2$ levels despite its smallest dissolved fraction based on Henry's law constants. Since its oxidation in the aqueous phase is faster than it is in the gas phase, the continuous removal from the gas phase by consumption in the aqueous phase leads to an efficient decrease of the $HO_2$ source. The contributions of the more soluble dialdehydes (glyoxal and methylglyoxal) to the $HO_2$ levels are marginal and only change predicted $HO_2$ concentrations by $\sim 1\%$ in total. Although the box model simulations performed in the present study might not be fully quantitative since the results depend on various conditions (e.g. drop distribution, liquid water content, processing time, impact of clouds on photolysis rates, etc.), it can be expected that the identified trends are robust. In general, these studies suggest that a very small ($< 1\%$) fraction of DOC might have significant impact on the oxidant levels in the atmospheric multiphase system.

**Supplementary material related to this article is available online at: http://www.atmos-chem-phys-discuss.net/12/33083/2012/acpd-12-33083-2012-supplement.pdf.**

*Acknowledgements.* BE acknowledges support from NOAA's Climate Goal. We are grateful to James Hutchings and Aurelie Marcotte for assistance with sampling during the fog and cloud field studies. We are grateful to Mike Mata, Qi Zhang and Cort Anastasio for help with the Davis field work and Juniper Buller for help with the Whistler field work. Funding for the research was provided by National Science Foundation grants AGS0847710, AGS 0907261 and Environment Canada through the Clean Air Regulatory Agenda. The statements and conclusions in this paper are those of the authors and not necessarily those of NSF or Environment Canada. The mention of commercial products, their source, or their use in connection with material reported herein is not to be construed as actual or implied endorsement of such products.





ACPD
12, 33083–33125, 2012



## References


Anastasio, C., Faust, B. C., and Allen, J. M.: Aqueous phase photochemical formation of hydrogen peroxide in authentic cloud waters, J. Geophys. Res., 99, 8231–8248, doi:10.1029/94jd00085, 1994.

Axson, J. L., Takahashi, K., De Haan, D. O., and Vaida, V.: Gas-phase water-mediated equilibrium between methylglyoxal and its geminal diol, P. Natl. Acad. Sci. USA, 107, 6687–6692, doi:10.1073/pnas.0912121107, 2010.

Baboukas, E. D., Kanakidou, M., and Mihalopoulos, N.: Carboxylic acids in gas and particulate phase above the Atlantic Ocean, J. Geophys. Res., 105, 14459–14471, 2000.

Bauer, H., Kasper-Giebl, A., Löflund, M., Giebl, H., Hitzenberger, R., Zibuschka, F., and Puxbaum, H.: The contribution of bacteria and fungal spores to the organic carbon content of cloud water, precipitation and aerosols, Atmos. Res., 64, 109–119, doi:10.1016/s0169-8095(02)00084-4, 2002.

Betterton, E. A. and Hoffmann, M. R.: Henry's law constants of some environmentally important aldehydes, Environ. Sci. Technol., 22, 1415–1418, 1988.

Betterton, E. A., Erel, Y., and Hoffmann, M.: Aldehyde-bisulfite adducts: prediction of some of their thermodynamic and kinetic properties, Environ. Sci. Technol., 22, 92–99, 1988.

Blando, J. D. and Turpin, B. J.: Secondary organic aerosol formation in cloud and fog droplets: a literature evaluation of plausibilty, Atmos. Environ., 34, 1623–1632, 2000.

Brüggemann, E., Gnauk, T., Mertes, S., Acker, K., Auel, R., Wieprecht, W., Möller, D., Collett Jr., J. L., Chang, H., Galgon, D., Chemnitzer, R., Rüd, C., Junek, R., Wiedensohler, A., and Herrmann, H.: Schmücke hill cap cloud and valley stations aerosol characterisation during FEBUKO (I): particle size distribution, mass, and main components, Atmos. Environ., 39, 4291–4303, doi:10.1016/j.atmosenv.2005.02.013, 2005.

Buxton, G. V., Malone, T. N., and Salmon, G. A.: Oxidation of glyoxal initiated by OH in oxygenated aqueous solutions, J. Chem. Soc. Faraday Trans., 93, 2889–2891, 1997.

Carrillo, J. H., Emert, S. E., Sherman, D. E., Herckes, P., and Collett Jr., J. L.: An economical optical cloud/fog detector, Atmos. Res., 87, 259–267, 2008.

Chameides, W. L.: The photochemistry of a remote marine stratiform cloud, J. Geophys. Res., 89, 4739–4755, 1984.

Chow, J. C., Watson, J. G., Lowenthal, D. H., Chen, L. W. A., and Magliano, K. L.: Particulate carbon measurements in California's San Joaquin Valley, Chemosphere, 62, 337–348, 2006.






ACPD
12, 33083–33125, 2012



Collett Jr., J. L., Herckes, P., Youngster, S., and Lee, T.: Processing of atmospheric organic matter by California radiation fogs, Atmos. Res., 87, 323–341, 2008.
Ehrenhauser, F. S., Khadapkar, K., Wang, Y., Hutchings, J. F., Delhomme, O., Kommalapati, R. R., Herckes, P., Wornat, M. J., and Valsaraj, K. T.: Processing of atmospheric polycyclic aromatic hydrocarbons by fog in an urban environment, J. Environ. Monitor., 14, 2566–2579, doi:10.1039/C2EM30336A, 2012.
Ervens, B., George, C., Williams, J. E., Buxton, G. V., Salmon, G. A., Bydder, M., Wilkinson, F., Dentener, F., Mirabel, P., Wolke, R., and Herrmann, H.: CAPRAM2.4 (MODAC mechanism): an extended and condensed tropospheric aqueous phase mechanism and its application, J. Geophys. Res., 108, D14, doi:10.1029/2002JD002202, 2003a.
Ervens, B., Herckes, P., Feingold, G., Lee, T., Collett, J. L. J., and Kreidenweis, S. M.: On the drop-size dependence of organic acid and formaldehyde concentrations in fog, J. Atmos. Chem., 46, 239–269, 2003b.
Ervens, B., Feingold, G., Frost, G. J., and Kreidenweis, S. M.: A modeling study of aqueous production of dicarboxylic acids, 1. chemical pathways and speciated organic mass production, J. Geophys. Res., 109, D15205, doi:10.1029/2003JD004387, 2004.
Ervens, B., Cubison, M. J., Andrews, E., Feingold, G., Ogren, J. A., Jimenez, J. L., DeCarlo, P., and Nenes, A.: Prediction of cloud condensation nucleus number concentration using measurements of aerosol size distributions and composition and light scattering enhancement due to humidity, J. Geophys. Res., 112, D10S32, doi:10.1029/2006JD007426, 2007.
Ervens, B., Turpin, B. J., and Weber, R. J.: Secondary organic aerosol formation in cloud droplets and aqueous particles (aqSOA): a review of laboratory, field and model studies, Atmos. Chem. Phys., 11, 11069–11102, doi:10.5194/acp-11-11069-2011, 2011.
Finlayson-Pitts, B. J. and Pitts, J. N.: Chemistry of the Upper and Lower Atmosphere, Academic Press, San Diego, California, 969 pp., 2000.
Fraser, M. P., Yue, Z. W., Tropp, R. J., Kohl, S. D., and Chow, J. C.: Molecular composition of organic fine particulate matter in Houston, Atmos. Environ., 36, 5751–5758, 2002.
Frost, G. J., Trainer, M., Mauldin III, R. L., Eisele, F. L., Prevot, A. S. H., Madronich, S., Kok, G., Schillawski, R. D., Baumgardner, D., and Bradshaw, J.: Photochemical modeling of OH levels during the first Aerosol Characterization Experiment (ACE 1), J. Geophys. Res., 104, 16041–16052, doi:10.1029/1999jd900171, 1999.





ACPD
12, 33083–33125, 2012



Fu, T., Jacob, D. J., Wittrock, F., Burrows, J. P., Vrekoussis, M., and Henze, D. K.: Global budgets of atmospheric glyoxal, methylglyoxal, and implications for formation of secondary organic aerosol, J. Geophys. Res., 113, D15303, doi:10.1029/2007JD009505, 2008.

Fuzzi, S. and Zappoli, S.: The organic component of fog droplets, In: Proceedings of the 10–12-th International Conference on Cloud and Precipitation, Zurich, Switzerland, 1077–1079, 1996.

Galloway, M. M., Huisman, A. J., Yee, L. D., Chan, A. W. H., Loza, C. L., Seinfeld, J. H., and Keutsch, F. N.: Yields of oxidized volatile organic compounds during the OH radical initiated oxidation of isoprene, methyl vinyl ketone, and methacrolein under high-$NO_x$ conditions, Atmos. Chem. Phys., 11, 10779–10790, doi:10.5194/acp-11-10779-2011, 2011.

Gong, W., Stroud, C., and Zhang, L.: Cloud processing of gases and aerosols in air quality modeling, Atmosphere, 2, 567–616, doi:10.3390/atmos2040567, 2011.

Guo, J., Wang, Y., Shen, X., Wang, Z., Lee, T., Wang, X., Li, P., Sun, M., Collett Jr., J. L., Wang, W., and Wang, T.: Characterization of cloud water chemistry at Mount Tai, China: seasonal variation, anthropogenic impact, and cloud processing, Atmos. Environ., 60, 467–476, doi:10.1016/j.atmosenv.2012.07.016, 2012.

Heald, C. L., Goldstein, A. H., Allan, J. D., Aiken, A. C., Apel, E., Atlas, E. L., Baker, A. K., Bates, T. S., Beyersdorf, A. J., Blake, D. R., Campos, T., Coe, H., Crounse, J. D., DeCarlo, P. F., de Gouw, J. A., Dunlea, E. J., Flocke, F. M., Fried, A., Goldan, P., Griffin, R. J., Herndon, S. C., Holloway, J. S., Holzinger, R., Jimenez, J. L., Junkermann, W., Kuster, W. C., Lewis, A. C., Meinardi, S., Millet, D. B., Onasch, T., Polidori, A., Quinn, P. K., Riemer, D. D., Roberts, J. M., Salcedo, D., Sive, B., Swanson, A. L., Talbot, R., Warneke, C., Weber, R. J., Weibring, P., Wennberg, P. O., Worsnop, D. R., Wittig, A. E., Zhang, R., Zheng, J., and Zheng, W.: Total observed organic carbon (TOOC) in the atmosphere: a synthesis of North American observations, Atmos. Chem. Phys., 8, 2007–2025, doi:10.5194/acp-8-2007-2008, 2008.

Healy, R. M., Wenger, J. C., Metzger, A., Duplissy, J., Kalberer, M., and Dommen, J.: Gas/particle partitioning of carbonyls in the photooxidation of isoprene and 1,3,5-trimethylbenzene, Atmos. Chem. Phys., 8, 3215–3230, doi:10.5194/acp-8-3215-2008, 2008.

Hennigan, C. J., Bergin, M. H., Russell, A. G., Nenes, A., and Weber, R. J.: Gas/particle partitioning of water-soluble organic aerosol in Atlanta, Atmos. Chem. Phys., 9, 3613–3628, doi:10.5194/acp-9-3613-2009, 2009.





ACPD
12, 33083–33125, 2012



Herckes, P., Lee, T., Trenary, L., Kang, G. U., Chang, H., and Collett, J. L.: Organic matter in San Joaquin Valley radiation fogs, Environ. Sci. Technol., 36, 4777–4782, 2002a.
Herckes, P., Hannigan, M. P., Trenary, L., Lee, T., and Collett, J. L.: The organic composition of radiation fog in Davis (California), Atmos. Res., 64, 99–108, 2002b.
Herckes, P., Chang, H., Lee, T., and Collett Jr., J. L.: Air pollution processing by radiation fogs, Water Air Soil Poll., 181, 65–75, 2007.
Herrmann, H., Tilgner, A., Barzaghi, P., Majdik, Z., Gligorovski, S., Poulain, L., and Monod, A.: Towards a more detailed description of tropospheric aqueous phase organic chemistry: CAPRAM 3.0, Atmos. Environ, 39, 4351–4363, 2005.
Igawa, M., Munger, J. W., and Hoffmann, M. R.: Analysis of aldehydes in cloud- and fogwater samples by HPLC with a postcolumn reaction detector, Environ. Sci. Technol., 23, 556–561, 1989.
Ip, H. S. S., Huang, X. H. H., and Yu, J. Z.: Effective Henry's law constants of glyoxal, glyoxylic acid and glycolic acid, Geophys. Res. Lett., 36, L01802, doi:10.1029/2008GL036212, 2009.
Khare, P., Kumar, N., Kumari, K. M., and Srivastava, S. S.: Atmospheric formic and acetic acids: an overview, Rev. Geophys., 37, 227–248, 1999.
Khwaja, H. A., Brudnoy, S., and Husain, L.: Chemical characterization of 3 summer cloud episodes at Whiteface Mountain, Chemosphere, 31, 3357–3381, 1995.
Lee, A. K. Y., Herckes, P., Leaitch, W. R., Macdonald, A. M., and Abbatt, J. P. D.: Aqueous OH oxidation of ambient organic aerosol and cloud water organics: formation of highly oxidized products, Geophys. Res. Lett., 38, L11805, doi:10.1029/2011gl047439, 2011.
Lee, A. K. Y., Hayden, K. L., Herckes, P., Leaitch, W. R., Liggio, J., Macdonald, A. M., and Abbatt, J. P. D.: Characterization of aerosol and cloud water at a mountain site during WACS 2010: secondary organic aerosol formation through oxidative cloud processing, Atmos. Chem. Phys., 12, 7103–7116, doi:10.5194/acp-12-7103-2012, 2012.
Lelieveld, J. and Crutzen, P. J.: The role of clouds in tropospheric photochemistry, J. Atmos. Chem., 12, 229–268, 1991.
Li, S.-M., Macdonald, A. M., Leithead, A., Leaitch, W. R., Gong, W., Anlauf, K. G., Toom-Sauntry, D., Hayden, K., Bottenheim, J., and Wang, D.: Investigation of carbonyls in cloud water during ICARTT, J. Geophys. Res., 113, D17206, doi:10.1029/2007JD009364, 2008.
Lim, Y. B., Tan, Y., Perri, M. J., Seitzinger, S. P., and Turpin, B. J.: Aqueous chemistry and its role in secondary organic aerosol (SOA) formation, Atmos. Chem. Phys., 10, 10521–10539, doi:10.5194/acp-10-10521-2010, 2010.





ACPD
12, 33083–33125, 2012



Limbeck, A. and Puxbaum, H.: Dependence of in-cloud scavenging of polar organic aerosol compounds on the water solubility, J. Geophys. Res., 105, D15, 19857–19867, 2000.
Lin, Y. C., Schwab, J. J., Demerjian, K. L., Bae, M.-S., Chen, W.-N., Sun, Y., Zhang, Q., Hung, H.-M., and Perry, J.: Summertime formaldehyde observations in New York City: ambient levels, sources and its contribution to $HO_x$ radicals, J. Geophys. Res., 117, D08305, doi:10.1029/2011jd016504, 2012.
Loeflund, M., Kasper-Giebel, A., Schuster, B., Giebl, H., Hitzenberger, R., and Puxbaum, H.: Formic, acetic, oxalic, malonic and succinic acid concentrations and their contribution to organic carbon in cloud water, Atmos. Environ., 26, 1553–1558, 2002.
Macdonald, A. M., Leaitch, W. R., Abbatt, J. P. D., Ahlm, L., Al-Basheer, W., Betram, A. K., Buller, J., Campuzano-Jost, P., Chan, E., Corbin, J., Cziczo, D., Elford, A., Hayden, K. A., Herckes, P., Lee, A. K. Y., Li, S.-M., Liggio, J., Liu, P. S. K., Mihele, C., Noone K. J., Pierce, J. R., Russell, L. M., Toom-Sauntry, D., Schroder, J., Sharma, S., Sheppard, A., Sjostedt, S. J., Slowik, J. G., Strawbridge, K., Stupple, G., Vlasenko, A., Wainwright, C., Wang, Y., Wentzell, J., Wiebe, H. A., and Wong, J. P. S.: An overview of the 2010 WACS2010: biogenic aerosol formation, mountain flows and CCN, Atmos. Chem. Phys. Discuss., in preparation, 2012.
Madronich, S. and Calvert, J. G.: Permutation reactions of organic peroxy radicals in the troposphere, J. Geophys. Res., 95, 5697–5715, 1990.
Maria, S. F. and Russell, L. M.: Organic and inorganic aerosol below-cloud scavenging by suburban New Jersey precipitation, Environ. Sci. Technol., 39, 4793–4800, doi:10.1021/es0491679, 2005.
Maroń, M. K., Takahashi, K., Shoemaker, R. K., and Vaida, V.: Hydration of pyruvic acid to its geminal-diol, 2,2-dihydroxypropanoic acid, in a water-restricted environment, Chem. Phys. Lett., 513, 184–190, doi:10.1016/j.cplett.2011.07.090, 2011.
Matsumoto, K., Kawai, S., and Igawa, M.: Dominant factors controlling concentrations of aldehydes in rain, fog, dew water, and in the gas phase, Atmos. Environ., 39, 7321–7329, doi:10.1016/j.atmosenv.2005.09.009, 2005.
Matsunaga, S. N., Kato, S., Yoshino, A., Greenberg, J. P., Kajii, Y., and Guenther, A. B.: Gas-aerosol partitioning of semi volatile carbonyls in polluted atmosphere in Hachioji, Tokyo, Geophys. Res. Lett., 32, L11805, doi:10.1029/2004gl021893, 2005.





ACPD
12, 33083–33125, 2012



Mayer, B., Kylling, A., Madronich, S., and Seckmeyer, G.: Enhanced absorption of UV radiation due to multiple scattering in clouds: experimental evidence and theoretical explanation, J. Geophys. Res., 103, 31241–31254, doi:10.1029/98jd02676, 1998.

Monod, A., Poulain, L., Grubert, S., Voisin, D., and Wortham, H.: Kinetics of OH-initiated oxidation of oxygenated organic compounds in the aqueous phase: new rate constants, structure-activity relationships and atmospheric implications, Atmos. Environ., 39, 7667–7688, 2005.

Morita, A., Kanaya, Y., and Francisco, J. S.: Uptake of the $HO_2$ radical by water: molecular dynamics calculations and their implications for atmospheric modeling, J. Geophys. Res., 109, D09201, doi:10.1029/2003jd004240, 2004.

Müller, K., van Pinxteren, D., Plewka, A., Svrcina, B., Kramberger, H., Hofmann, D., Bächmann, K., and Herrmann, H.: Aerosol characterisation at the FEBUKO upwind station Goldlauter (II): detailed organic chemical characterisation, Atmos. Environ., 39, 4219–4231, doi:10.1016/j.atmosenv.2005.02.008, 2005.

Munger, J. W., Collett, J., Daube, B. C., and Hoffmann, M. R.: Carboxylic acids and carbonyl compounds in southern California clouds and fogs, Tellus B, 41, 230–242, doi:10.1111/j.1600-0889.1989.tb00303.x, 1989.

Munger, J. W., Jacob, D. J., Daube, B. C., Horowitz, L. W., Keene, W. C., and Heikes, B. C.: Formaldehyde, glyoxal and methylglyoxal at a rural mountain site in central Virginia, J. Geophys. Res., 100, 9325–9333, 1995.

Ng, N. L., Canagaratna, M. R., Jimenez, J. L., Chhabra, P. S., Seinfeld, J. H., and Worsnop, D. R.: Changes in organic aerosol composition with aging inferred from aerosol mass spectra, Atmos. Chem. Phys., 11, 6465–6474, doi:10.5194/acp-11-6465-2011, 2011.

Nishino, N., Arey, J., and Atkinson, R.: Formation yields of glyoxal and methylglyoxal from the gas-phase OH radical-initiated reactions of toluene, xylenes, and trimethylbenzenes as a function of $NO_2$ concentration, J. Phys Chem. A, 114, 10140–10147, doi:10.1021/jp105112h, 2010.

Olson, T. M. and Hoffmann, M. R.: Hydroxyalkylsulfonate formation: its role as a S(IV) reservoir in atmospheric water droplets, Atmos. Environ., 23, 985–997, 1989.

Plum, C. N., Sanhueza, E., Atkinson, R., Carter, W. P. L., and Pitts Jr., J. N.: OH radical rate constants and photolysis rates of “alpha”-dicarbonyls, Environ. Sci. Technol., 17, 479–484, 1983.

Raja, S., Raghunathan, R., Yu, X.-Y., Lee, T., Chen, J., Kommalapati, R. R., Murugesan, K., Shen, X., Qingzhong, Y., Valsaraj, K. T., and Collett Jr., J. L.: Fog chem-





ACPD
12, 33083–33125, 2012



istry in the Texas–Louisiana gulf coast corridor, Atmos. Environ., 42, 2048–2061, doi:10.1016/j.atmosenv.2007.12.004, 2008.
Raja, S., Raghunathan, R., Kommalapati, R. R., Shen, X., Collett Jr., J. L., and Valsaraj, K. T.: Organic composition of fogwater in the Texas–Louisiana gulf coast corridor, Atmos. Environ., 43, 4214–4222, doi:10.1016/j.atmosenv.2009.05.029, 2009.
Rao, X. and Collett, J. L.: The drop size-dependence of iron and manganese in clouds and fogs: implications for sulfate production, J. Atmos. Chem., 30, 273–289, 1998.
Reilly, J. E., Rattigan, O. V., Moore, K. M., Judd, C., Sherman, D. E., Dutkiewicz, V. A., Kreidenweis, S. M., Husain, L., and Collett, J. L.: Drop size dependent S(IV) oxidation in chemically heterogenous radiation fogs, Atmos. Environ., 35, 5717–5728, 2001.
Schaefer, T., Schindelka, J., Hoffmann, D., and Herrmann, H.: Laboratory kinetic and mechanistic studies on the OH-initiated oxidation of acetone in aqueous solution, J. Phys. Chem. A, 116, 6317–6326, doi:10.1021/jp2120753, 2012.
Schwab, J. J., Felton, H. D., and Demerjian, K. L.: Aerosol chemical composition in New York state from integrated filter samples: urban/rural and seasonal contrasts, J. Geophys. Res., 109, D16S05, doi:10.1029/2003jd004078, 2004.
Seinfeld, J. H. and Pandis, S. N.: Atmospheric Chemistry and Physics, John Wiley & Sons, New York, 1326 pp., 1998.
Slowik, J. G., Wong, J. P. S., and Abbatt, J. P. D.: Real-time, controlled OH-initiated oxidation of biogenic secondary organic aerosol, Atmos. Chem. Phys., 12, 9775–9790, doi:10.5194/acp-12-9775-2012, 2012.
Spaulding, R. S., Schade, G. W., Goldstein, A. H., and Charles, M. J.: Characterization of secondary atmospheric photooxidation products: evidence of biogenic and anthropogenic sources, J. Geophys. Res., 108, D8, doi:10.1029/2002JD002478, 2003.
Straub, D. J., Hutchings, J. W., and Herckes, P.: Measurements of fog composition at a rural site, Atmos. Environ., 47, 195–205, doi:10.1016/j.atmosenv.2011.11.014, 2012.
Stroud, C., Madronich, S., Atlas, E., Ridley, B., Flocke, F., Weinheimer, A., Talbot, R., Fried, A., Wert, B., Shetter, R., Lefer, B., Coffey, M., Heickes, B., and Blake, D.: Photochemistry in the Arctic free troposphere: $NO_x$ budget and the role of odd nitrogen reservoir recycling, Atmos. Environ., 37, 3351–3364, 2003.
Tie, X., Madronich, S., Walters, S., Zhang, R., Rasch, P., and Collins, W.: Effects of clouds on photolysis and oxidants in the troposphere, J. Geophys. Res., 108, D20, doi:10.1029/2003JD003659, 2003.





ACPD
12, 33083–33125, 2012



van Pinxteren, D., Plewka, A., Hofmann, D., Müller, K., Kramberger, H., Svrinca, B., Bächmann, K., Jaeschke, W., Mertes, S., Collett, J. L., and Herrmann, H.: Schmücke hill cap cloud and valley stations aerosol characterisation during FEBUKO (II): organic compounds, Atmos. Environ., 39, 4305–4320, 2005.

Wang, G., Kawamura, K., Xie, M., Hu, S., Li, J., Zhou, B., Cao, J., and An, Z.: Selected water-soluble organic compounds found in size-resolved aerosols collected from urban, mountain and marine atmospheres over East Asia, Tellus B, 63, 371–381, doi:10.1111/j.1600-0889.2011.00536.x, 2011.

Wang, Z., Wang, T., Guo, J., Gao, R., Xue, L., Zhang, J., Zhou, Y., Zhou, X., Zhang, Q., and Wang, W.: Formation of secondary organic carbon and cloud impact on carbonaceous aerosols at Mount Tai, North China, Atmos. Environ., 46, 516–527, doi:10.1016/j.atmosenv.2011.08.019, 2012.

Warneck, P.: Multi-phase chemistry of $C_2$ and $C_3$ organic compounds in the marine atmosphere, J. Atmos. Chem, 51, 119–159, 2005.

Yin, Y., Parker, D. J., and Carslaw, K. S.: Simulation of trace gas redistribution by convective clouds – Liquid phase processes, Atmos. Chem. Phys., 1, 19–36, doi:10.5194/acp-1-19-2001, 2001.

Zhang, Q., Worsnop, D. R., Canagaratna, M. R., and Jimenez, J. L.: Hydrocarbon-like and oxygenated organic aerosols in Pittsburgh: insights into sources and processes of organic aerosols, Atmos. Chem. Phys., 5, 3289–3311, doi:10.5194/acp-5-3289-2005, 2005.

Zhou, X. and Mopper, K.: Apparent partition coefficients of 15 carbonyl compounds between air and seawater and between air and freshwater; implications for air-sea exchange, Environ. Sci. Technol., 24, 1864–1869, 1990.





ACPD
12, 33083–33125, 2012



**Table 1.** Overview of LWC and DOC concentrations at various locations. Based on these values, together with estimated TOOC levels, the organic fraction in the aqueous phase and the effective Henry's law constant for DOC ($K_H^{*DOC}$, Eq. 1) have been calculated.

| Location | LWC | DOC | | OC in the particle phase $OC_p$ | Reference | TOOC[a] | Organic fraction in the aqueous phase $F(OC_{aq})$ [%] | $K_H^{*DOC}$ |
|---|---|---|---|---|---|---|---|---|
| | $g\,m^{-3}$ | $mg\,C\,L_{aq}^{-1}$ | $\mu g\,C\,m^{-3}$ | $\mu g\,C\,m^{-3}$ | | $\mu g\,C\,m^{-3}$ | | $10^4\,M\,atm^{-1}$ |
| Fresno, CA | 0.069[b] | 12.4 | 0.85 | 9.0 | DOC: estimated based on (Chow et al., 2006) | 73.3 | 1 % | 0.7 |
| Mount Tai (China) | 0.25 | 18.5 | 4.6 | 5.5 | LWC: (Guo et al., 2012); DOC: (Wang et al., 2012) | 44.8 | 10 % | 1.9 |
| Davis, CA | 0.08 | 12.5 | 1.0 | 3.7 | This study | 30.1 | 3 % | 1.8 |
| Houston, TX | 0.065 | 10.4 | 0.68 | 3.2 | LWC: (Raja et al., 2009); DOC average from (Fraser et al., 2002) | 26.1 | 3 % | 1.7 |
| Whistler (Canada) | 0.2 | 4 | 0.8 | 2.6 | This study | 21.0 | 4 % | 0.8 |
| Angiola, CA | 0.21[b] | 6.9 | 1.5 | 2.5 | DOC estimated based on (Chow et al., 2006) | 20.4 | 7 % | 1.5 |
| Baton Rouge, LA | 0.08 | 5.3 | 1.6 | 2.4 | (Raja et al., 2009); annual mean from IMPROVE CSM | 19.5 | 2 % | 1.2 |
| Schmücke (Germany)[c] | 0.27 | 5.8 | 0.42 | 1.8 | (Brüggemann et al., 2005) | 15.0 | 11 % | 2.0 |
| Mount Rax (Austria) | 0.28 | 6.02 | 1.7 | 1.3 | (Bauer et al., 2002) | 10.2 | 17 % | 2.9 |
| Whiteface Mountain, NY | 0.49 | 7.6 | 3.7 | 1 | LWC: (Khwaja et al., 1995); DOC: estimated based on (Schwab et al., 2004) | 8.1 | 46 % | 7.1 |

[a] The TOOC values are estimated as for locations of similar pollutions levels, based on compilation by Heald et al. (2008), see text.
[b] unpublished LWC value.
[c] average of three cloud events.





ACPD
12, 33083–33125, 2012



**Table 2.** Initial mixing ratios [ppb] for box model simulations.

| | Whistler<br>Macdonald et al. (2012) | Davis<br>Ehrenhauser et al. (2012) |
|---|---|---|
| Isoprene | 0.6 | 0.2 |
| Benzene | 0.05 | 2 |
| Toluene | 0.1 | 4 |
| $O_3$ | 25 | 70 |
| $NO_x$ | 4 | 20 |
| CO | 120 | 500 |





ACPD
12, 33083–33125, 2012



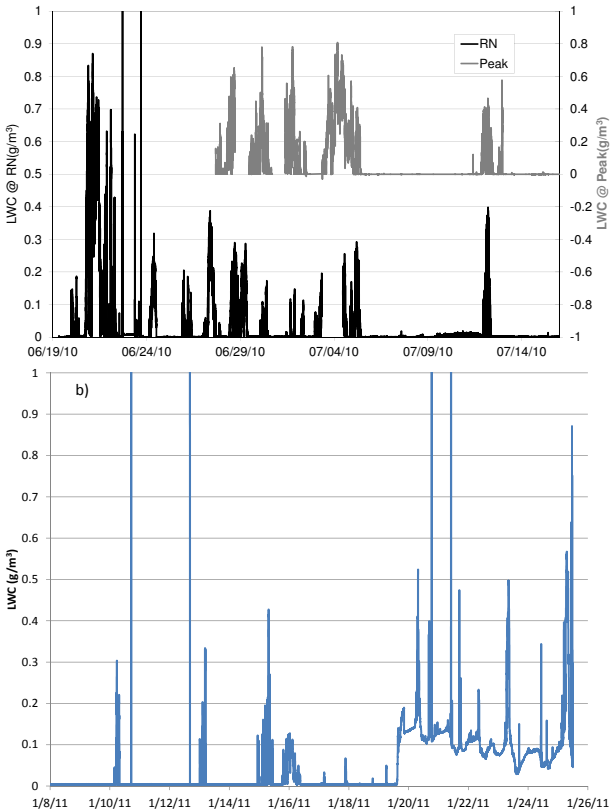


**Fig. 1.** Temporal evolution of liquid water content (LWC) **(a)** in Whistler (fog/intercepted clouds) at Raven's Nest (RN) and Whistler Peak, measured with Gerber PVM and **(b)** in Davis measured with a CSU-OFD.





ACPD
12, 33083–33125, 2012



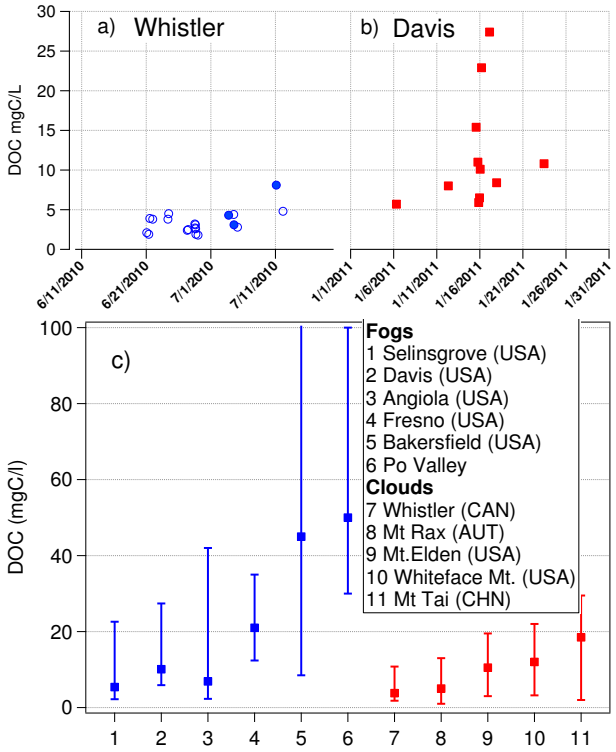


**Fig. 2.** Time series of dissolved organic carbon (DOC) concentrations in **(a)** Whistler cloud water (open dots correspond to samples from Raven's Nest side while full symbols represent samples from the Peak site) and **(b)** Davis fog water; **(c)** select DOC concentrations in fogs and clouds at several locations. Symbols represent median values, lines represent the range of values (min-max). (This study, Anastasio et al., 1994; Fuzzi and Zappoli, 1996; Loeflund et al., 2002; Herckes et al., 2007; Wang et al., 2011; Straub et al., 2012).





ACPD
12, 33083–33125, 2012



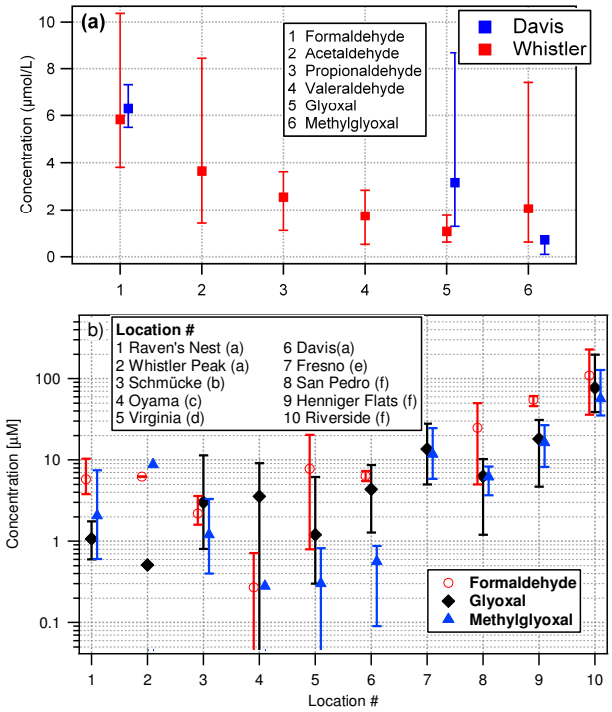


**Fig. 3. (a)** Measured aldehyde concentrations in cloud (Whistler, red) and fog water (Davis, blue) **(b)** Comparison to Formaldehyde, Glyoxal and Methylglyoxal concentrations at various locations: (a) this study; (b) (van Pinxteren et al., 2005); (c) (Matsumoto et al., 2005); (d) (Munger et al., 1995); (e) unpublished; (f) (Igawa et al., 1989).





ACPD
12, 33083–33125, 2012



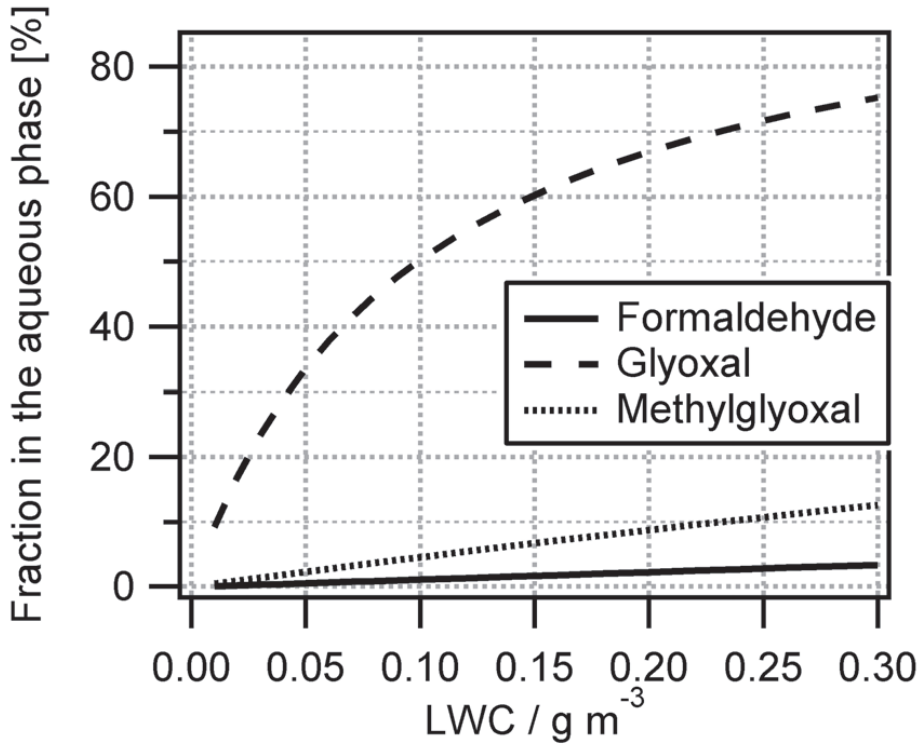


**Fig. 4.** Predicted dissolved aldehyde fraction in the aqueous phase as a function of liquid water content, assuming thermodynamic equilibrium and effective Henry's law constants (including hydration).





ACPD
12, 33083–33125, 2012



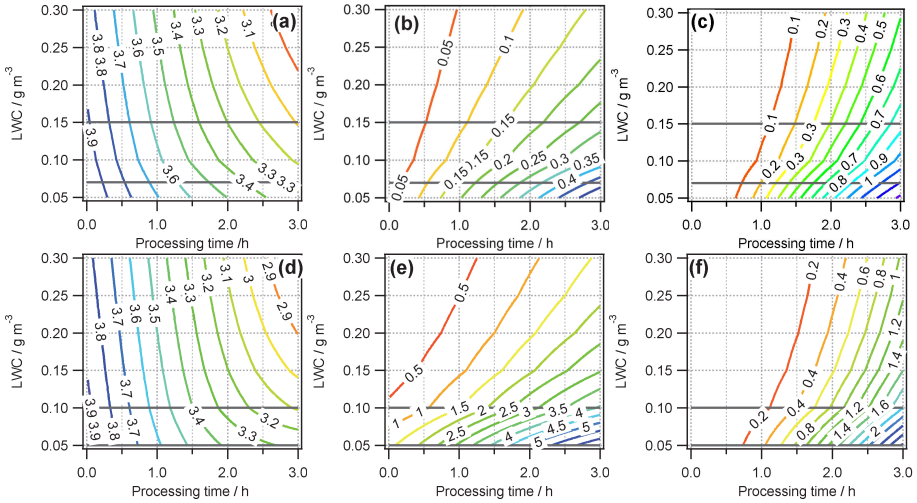


**Fig. 5.** Predicted concentrations of aldehydes [mg $L^{-1}$] in the aqueous phase for the conditions in Whistler (upper panel) and Davis (lower panel) as a function of LWC and processing time (assuming continuous gas/ aqueous phase interactions). **(a, d)** Formaldehyde; **(b, e)** Glyoxal; **(c, f)** Methylglyoxal; the grey lines show the LWC range as observed in Whistler and Davis, respectively.





ACPD
12, 33083–33125, 2012

The role of the aqueous phase in impacting trace gas budgets

B. Ervens et al.



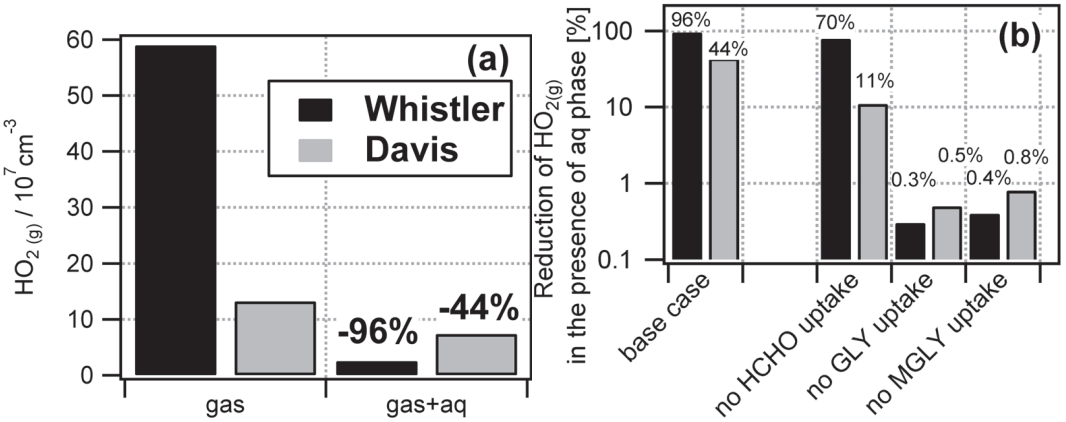


**Fig. 6.** Comparison of predicted $HO_2$(gas) concentrations in the presence and absence of an aqueous phase **(a)** Absolute $HO_2$(g) concentration [$cm^{-3}$] for a pure gas phase system ("gas") and the multiphase system ("gas + aq"); **(b)** reduction of $HO_2$(g) [%] (Eq. 5): "base case" refers to the simulations as in **(a)**; the other three sets of simulations ("no HCHO, no GLY, no MGLY uptake", respectively), refer to exploratory simulations where the uptake of a single aldehyde into the aqueous phase is excluded from the chemical mechanism in the multiphase (gas + aqueous) system.





ACPD
12, 33083–33125, 2012